PROPERTIES OF THE LUNAR EXOSPHERE DURING THE PERSEID 2009 METEOR SHOWER

Berezhnoy A.A.[a], Churyumov K.I.[b], Kleshchenok V.V.[b], Kozlova E.A.[a], Mangano V.[c], Pakhomov Yu.V.[d], Ponomarenko V.O.[b], Shevchenko V.V[a], Velikodsky Yu.I.[e]

[a]*Sternberg Astronomical Institute, Moscow State University, Universitetskij pr., 13, Moscow, 119991 Russia*
[b]*Astronomical Observatory, Kyiv Taras Shevchenko National University, Observatorna Street, 3, Kyiv, 04053 Ukraine*
[c]*INAF-IAPS (Institute of Astrophysics and Planetology from Space), via del Fosso del Cavaliere 100, 00133 Rome, Italy*
[d]*Institute of Astronomy, Russian Academy of Sciences, Pyatnitskaya Street 48, Moscow, 119017 Russia*
[e]*Institute of Astronomy, Kharkiv National University, Sumska Street 35, Kharkiv, 61022 Ukraine*

arXiv:1404.2075v1 [astro-ph.EP] 8 Apr 2014

Abstract

Influence of the meteoroid bombardment on properties of the lunar exosphere has been confirmed. Quick increase in the zenith column density of Na atoms above the lunar north pole on August 13, 2009 at 0–1 UT is detected and explained by numerous collisions of relatively small Perseid meteoroids (<1 kg) with the Moon during maximum of the Perseid meteor shower. New stringent upper limits of the column densities for Ca, Ba, and Ti atoms in the lunar exosphere are obtained as 5×10^7, 2.2×10^6, and 6.9×10^8 cm^{-2}, respectively. It is found that the content of impact-produced Ca and Al atoms in the lunar exosphere is depleted as compared to that of Na atoms.

Keywords:
Moon, Atmospheres, Composition, Meteors, Impact, processes

1. Introduction

Spectral lines of atoms of sodium and potassium were discovered in the lunar exosphere by Potter and Morgan (1988). The emission lines of neutral sodium were detected at distances of about 5 lunar radii from the center of the Moon on the sunward side and much fainter emission was detected at distances up to about 15–20 lunar radii on the antisunward side. The typical velocity of Na atoms in the extended lunar coma is about 2 km/s suggesting a high-energy source, such as impact vaporization of the regolith (Mendillo et al., 1991). The distribution of sodium in the lunar exosphere depends on solar zenith angle, suggesting that most sodium atoms are liberated from the lunar surface by solar photons or by solar wind impact, in contrast to a source driven by uniform micrometeoroid bombardment (Flynn and Mendillo, 1993; Mendillo et al., 1993).

Properties of the extended lunar sodium exosphere have been explained by a 15% contribution of sporadic micrometeoroid impact vaporization occurring uniformly over the lunar surface and an 85% contribution of photon-induced desorption dependent on solar zenith angle over the sunlit hemisphere (Mendillo et al., 1999). In particular, impact vaporization caused by collisions of sporadic meteoroids with the Moon may account for up to 50% of exospheric Na atoms over the terminator and poles (Sarantos et al., 2010). Increase in the content of sodium atoms in the lunar exosphere is expected during activity of main meteor showers due to increasing intensity of meteoroid bombardment. For example, a small increase in temperature and column density of Na atoms in the lunar exosphere was detected during Leonid 1995 and 1997 showers (Hunten et al., 1998; Verani et al., 1998), but no similar effects were detected during Geminid 1999 and Quadrantid 1999 meteor showers (Barbieri et al., 2001; Verani et al., 2001). A bright Na spot in the lunar orbit was detected after maximum of the Leonid 1998 meteor shower (Smith et al., 1999). Thus, meteoroid impacts may lead to the production of Na atoms which are able to escape the lunar exosphere.

Several other authors reported sudden changes in the properties of the sodium lunar exosphere which may be associated with impacts of meteoroids. Hunten et al. (1991) detected an increase in the column density of Na atoms at 801 south latitude in the lunar exosphere of about 60% on October 14, 1990 as compared to the observations of October 12 and 13, 1990 while measurements at the equator showed no substantial change. These results were explained by the action of an unknown low-speed meteor shower. Similar quick changes in the column density of Na atoms above the north pole of the Moon on September 18–19, 1995, were reported and explained by impacts of numerous small low-speed meteoroids by Sprague et al. (1998). Sudden significant changes in Na temperature were detected during observations of the lunar poles on April 19 and May 10, 1998, which were interpreted as possible impacts of meteoroids (Sprague et al., 2012). These possible impacts may be associated with Lyrid (maximum on April 22) and η-Aquarid (maximum on May 6) meteor showers. Thus, the column density of Na atoms in the lunar exosphere at the poles varies significantly, but the nature of this variability remains poorly understood.

The atoms of refractory elements, such as Ca, Mg, Al, and

Table 1: Parameters of spectral observations of Na atoms in the lunar exosphere on August 12–14, 2009. The values of N_{zen0} are calculated at the assumed temperature of 3000 K and averaged from analysis of both Na (5890 and 5896 Å) lines. The accuracies of the values of observed intensities I_{obs} and the surface zenith column densities N_{zen0} are given at the 3 sigma level.

Time of observations UT	Illuminated fraction, (%)	Distance from the surface, (km)	Position angle (deg)	Intensity of Na D2 line, (R)	Intensity of Na D1 line, (R)	N_{zen0}(Na) (cm^2)
Aug.12, 23:13–23:43	58.8	90	18.9	146±6	68±6	$(8.2\pm0.5)\times10^8$
Aug.12, 23:54–Aug.13, 0:24	58.5	270	18.8	159±3	77±3	$(1.23\pm0.04)\times10^9$
Aug.13, 0:43–1:13	58.2	455	18.7	137±3	64±3	$(1.33\pm0.04)\times10^9$
Aug.13, 23:22–23:52	48	90	15.2	152±3	74±3	$(8.5\pm0.3)\times10^8$
Aug.13, 23:53–Aug.14, 0:23	47.7	270	15.1	136±3	66±3	$(1.00\pm0.04)\times10^9$
Aug.14, 0:26–0:56	47.4	455	15.0	89±3	45±3	$(8.7\pm0.5)\times10^8$

Fe, have not been detected in the lunar exosphere yet, while Mg and Ca atoms in the Hermean exosphere have, and their presence is explained by the action of high-energy mechanisms such as solar wind sputtering (Sarantos et al., 2011; Burger et al., 2012). Several attempts to detect atoms of refractory elements in the lunar exosphere have been performed (Flynn and Stern, 1996; Stern et al., 1997; Halekas et al., 2013; Cook et al., 2013), but all these observations were performed in the absence of main meteor showers. For this reason, meteoroid impacts were not considered in these papers as a source of the lunar exosphere. The search for lines of refractory elements above the north pole of the Moon during the Perseid 2009 meteor shower was performed by Churyumov et al. (2012), and preliminary results of these observations were reported. The mass of impacted Perseid meteoroids was estimated as 15 kg. The upper limits of Ca, Ba, and Ti atoms in the lunar exosphere were estimated using a simple barometric model as 1.6×10^7, 7.4×10^5, and $1.2\times10^7 cm^{-2}$, respectively. However, in this paper we use the more appropriate model of Chamberlain (1963) for the study of exospheric atoms. In addition, we also include a geometric factor in the data analysis, and re-analyze original observational data against the early paper of Churyumov et al. (2012).

2. Observations of the lunar exosphere and data reduction

Spectroscopic observations of NaI D1 (5895.9 Å) and D2 (5890.0 Å) resonance lines in the lunar exosphere were performed on August 12/13 and 13/14, 2009, during maximum of the Perseid meteor shower using the echelle spectrograph MMCS (Multi Mode Cassegrain Spectrometer) of the 2-m Zeiss telescope (Terskol branch of Institute of Astronomy of Russian Academy of Sciences, Kabardino-Balkaria, Russia). The slit of the spectrograph has a height of 1000 and a width of 200 . Using a 1245×1152 pixel CCD, 31 spectral orders in the range from 3720 to 7526 Å were recorded. The spectrograph resolution was R=13 500; the signal-to-noise ratio of the obtained spectra was about 50 at the position of NaI D2 line. Six echelle spectra were recorded at the distances of 50″, 150″, and 250″ (90, 270, and 455 km, respectively) from the lunar limb above the north pole which was bombarded by Perseid's meteoroids (see Table 1). The exposure time of each spectrum τ_{obs} was 1800 s.

The echelle package of the MIDAS software system was used to process the spectroscopic data reduction: remove the cosmic rays, detect and extract the echelle orders, wavelength calibrate using the spectrum of a standard Fe–Ar lamp, and flux calibrate using the standard star HD 214923. At the end of data reduction processing we obtain the spectra in absolute fluxes. At this stage, the data contained both the spectra of the lunar exosphere and the solar spectra reflected from the lunar surface and scattered in the Earth's atmosphere. To finally extract the contribution of the lunar exosphere we use the solar spectrum taken as the spectrum of daytime scattered light (see Fig. 1).

The spectral transparency of Earth's atmosphere at 600 nm was taken as 88% at 451 in accordance with Tug (1977). In Table 1, parameters of the performed observations are listed: the time of observations, the altitude of the slit above the lunar surface, the position angle of the observed point with respect to the direction of the north pole of the Moon, and the intensity of sodium resonance lines. We notice that: (1) the brightness of Na lines at 270 and 455 km from the limb is 109% and 93% versus that at 90 km on August 12/13, 2009 (see Fig. 1); (2) the brightness of Na lines at 270 and 455 km from the limb is 89% and 58% versus that at 90 km on August 13/14, 2009; (3) the brightness of the reflected solar spectrum at 270 and 455 km versus that at 90 km is 78% and 56% on August 12/13 and 73% and 52% on August 13/14, 2009, respectively. Similar behavior of the intensity of the scattered light in the vicinities of the Moon means that transparency of Earth's atmosphere was almost the same during both observational nights. More detailed information about properties of Na exosphere can be obtained from estimates of temperature and column density of Na atoms.

3. The properties of the lunar exosphere

Let us define the observed point as the nearest point at the line of sight to the lunar surface. According to Eq. (6.2.3) of Chamberlain and Hunten (1987) in approximation of optically thin atmosphere the line-of-sight column abundances N_{LOS} at the given altitude h of the observed point are calculated as

$$N_{LOS}(h) = 4\times10^6 \frac{\pi I}{g}, \quad (1)$$

where $4\pi I$ is the emission of atoms for the studied elements (in Rayleighs) measured at the altitude h and g is the emission rate factor in photons $atom^{-1}s^{-1}$ (see Table 2).

To theoretically model the properties of non-stationary exospheres, advanced Monte Carlo technique can be applied (see,

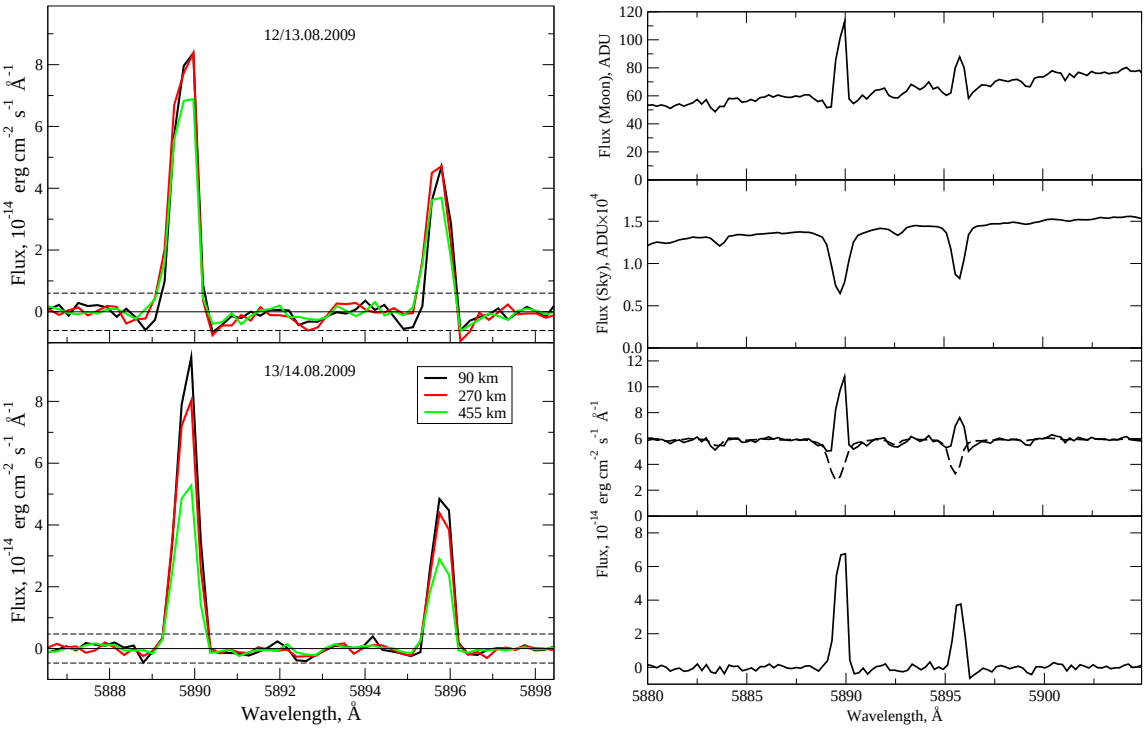

Figure 1: Spectra of Na lines in the lunar exosphere recorded on August 12/13 and August 13/14, 2009 (left). On the right: the sequence of data processing for the spectrum, recorded on August 13, 0:43–1:13 UT, is presented. From top to bottom: raw spectrum of the vicinities of the Moon in units of ADU (analog to digital unit), raw daytime spectrum of the sky (equivalent of the solar spectrum), calibrated spectra of the vicinities of the Moon and daytime sky spectrum (scaled to the first), and extracted spectrum of the lunar exosphere.

for example, Goldstein et al. (2001)). However, lack of information about exact positions, times, and masses of impacting meteoroids severely restricts usage of such models. For this reason, as a first step of interpretation of our observations, we assume local equilibrium of the exosphere. In this case we can use the sphericalsymmetry model of Chamberlain (1963) taking into account changes in gravity with height or, in some approximation, the simple barometric formula (in our range of altitudes) to obtain exospheric parameters near the observed point from line-of-sight column abundances. As a result the scale height H of Na atoms on August 13/14 is estimated as 700 7200 km using the least-squares regression of the measured intensities of Na D1 and D2 lines with theoretical exponential dependence of the intensity on height (the coefficient of determination r^2=0.9). The temperature of Na atoms is estimated as 3100±800 K from the barometric formula $T = HA_r(Na)a/R$, where the atomic mass $A_r(Na) = 0.023$ kg/mol, $a = 1.62$ m/s^2 is the gravitational acceleration on the surface of the Moon, and R=8.31 J mol^{-1}K^{-1} is the gas constant. For observations of August 12/13 the coefficient of determination r^2 is very low, about 0.1, and the temperature of Na atoms is estimated in the range between 18,000 and 7000 K. Hence, the temperature of Na atoms on August 12/13 cannot be estimated because during observations the column density of Na atoms changes significantly. Meteoroid bombardment is considered as the main source of Na atoms at the poles (Sarantos et al., 2010). In this paper the temperature of Na atoms is estimated to be about 3000 K when influence of meteoroid bombardment on properties of the lunar exosphere is maximal, because this time the Moon is located in the Earth's magnetosphere protecting the lunar surface from the interaction with solar wind particles. For these reasons, the temperature of Na atoms on August 12/13, 2009, is assumed to be the same (3100 K) as that on August 13/14, 2009.

We study several possible models of temporal activity of the Perseid meteor shower (see Fig. 2). In accordance with Chamberlain (1963) and assuming the local spherical symmetry of the exosphere (the case of numerous impacts of small meteoroids) the zenith column density $N_{zen}(h)$ at the given altitude h is estimated as

$$N_{zen} = \frac{1}{2} N_{LOS}(h) \frac{K_{zen}(R_{Moon}/H(h))}{K_{tan}(R_{Moon}/H(h))} \quad (2)$$

where $R_{Moon} = 1738$ km is the radius of the Moon, $H(h)$ is the scale height of studied species at the given altitude h in the lunar atmosphere, K_{zen} and K_{tan} are correction factors to the simple plane-parallel model of the lunar exosphere with constant gravity for calculations of $N_{zen}(h)$ and $N_{tan}(h)$, respectively, taken from Table 3 of Chamberlain (1963). According to Chamberlain (1963), the surface zenith column density N_{zen0} is calculated as

$$N_{zen0} = N_{zen}(h) \frac{e^{h/H(h)}}{1 + (h/R_{Moon})} \frac{\zeta_0(R_{Moon}/H_0) K_{zen0}(R_{Moon}/H_0)}{\zeta(R_{Moon}/H(h)) K_{zen}(R_{Moon}/H(h))} \quad (3)$$

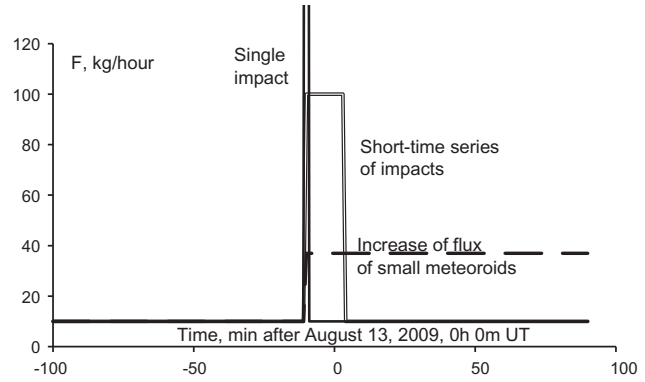

Figure 2: Models of activity of the Perseid meteor shower during observations of August 12/13, 2009.

Table 3: Solar wind density and velocity (ACE-SWEPAM, 2009; OMNI, 2009) and solar F10.7 index measurements (Space weather, 2009) on August 12–14, 2009.

Date UT	Solar wind density, (cm^{-3})	Solar wind velocity, (km/s)	Solar F10.7 cm flux, (10^{-22} J s^{-1} m^{-2} Hz^{-1})
Aug 12, 23:13 - Aug. 13, 01:13	5±1	(340-360)±3	66.5
Aug 13, 23:22 - Aug. 14, 00:56	5±2	(325-335)±2	66.8

where H_0 is the surface scale height, ζ is the partition function taken from Table 2 of Chamberlain (1963), the index "0" denotes the value of these considered functions at the surface. Let us suppose that the observed increase in the Na surface zenith column density (see Table 1) on August 12/13, 2009 is caused by numerous impacts of Perseid meteoroids. In this case the surface column density of additional impact-produced Na atoms $N_{zenImp0}$ can be estimated as

$$N_{zenImp0} = N_{zen0}(90) - N_{zen0}(270) \quad (4)$$

where $N_{zen0}(90)$ is the first spectrum obtained at 90 km $N_{zen0}(270)$ is the second spectrum obtained at 270 km

Here we use the approximation of the local equilibrium of the exosphere before and after meteoroid impacts. The $N_{zenImp0}$ value weakly depends on assumed temperature of Na atoms. Namely, this value is about $(4.9\pm0.8)\times10^8$, $(4.0\pm0.6)\times10^8$, and $(3.7\pm0.5)\times10^8$ cm^{-2} at temperature equal to 2000, 3000, and 4000 K, respectively. The found column density of Perseid impact produced Na atoms at the assumed temperature of 3100 K, about 4×10^8 cm^{-2}, is several times lower than the background column density of Na atoms above the north pole of the Moon near the last quarter, about 10^9 cm^{-2}, in agreement with our observations (see Table 2) and observations of Sprague et al. (2012), and comparable to the upper limit of the column density of impact-induced Na atoms delivered to the lunar exosphere by impacts of sporadic meteoroids, about 3×10^8 cm^{-2}, as estimated by Sarantos et al. (2008).

Taking into account the global asymmetry of the distribution of impact-produced Na atoms in the lunar exosphere, the mass of impact-produced Na atoms $M_{ImpProd}$ is estimated as

$$M_{ImpProd} = \frac{N_{zenImp0obs} A_r(Na) S_{bomb}}{k_{geom} N_A} \quad (5)$$

where $S_{bomb} = 1.9\times10^{17}$ cm^2 is the area of the hemisphere bombarded by the Perseid meteor shower (see Fig. 3), $N_A = 6.02\times10^{23}$ is the Avogadro constant, k_{geom} is the geometrical factor depending on the spatial distribution of emitting atoms in the lunar exosphere. The k_{geom} value is the ratio of the column density $N_{zenImp0obs}$ at the observed point to the average column density $N_{zenImp0}$ above the hemisphere bombarded by Perseids:

$$k_{geom} = \frac{2\pi f_N(b,l)}{\oint f_N(b,l) d\Omega}, \quad (6)$$

where the model distribution function $f_N(b,l)$ is the surface column density of impact-produced atoms of considered elements at given selenographic latitude b and longitude l while the integral is taken over the whole lunar surface. To model the distribution function $f_N(b,l)$, we use a simple approximation of homogeneous meteor shower with large numbers of meteoroid impacts and small impact-produced clouds. It was assumed that the activity of the Perseid meteor shower quickly increased soon after recording of the first spectrum and remained constant during recording of the second and third spectrum of August 12/13, 2009 (see also Fig. 2 and Section 4.3 of this paper), because the activity of the Perseid 2009 meteor shower on Earth might change quickly at the time scale of about 30 min (IMO, 2009). According to the simulation of impact-produced lunar exosphere performed by Goldstein et al. (2001) the surface column density decreases from impact point sharply, and most of mass of impact-produced matter concentrates in the small neighborhood of impact points during first hour after an impact. In this case it is safe to consider the global distribution function f_N is to be proportional to the frequency of meteoroid impacts, i.e. to cosine of angular distance ϕ from subradiant point on the hemisphere facing the radiant:

$$f_N(\phi) = f_0 cos(\phi) \quad (7)$$

and zero on another hemisphere. As a result, k_{geom}=2 cosϕ_{obs}, where ϕ_{obs} is the value of angle ϕ for the observed point. The angle ϕ_{obs} is equal to 56 and 59°; k_{geom} value is about 1.1 and 1.0 for observations of August 12/13 and 13/14, 2009, respectively. By using Eq. (5), the mass of additional impact-produced Na atoms is estimated as 3 kg.

We assume this additional mass is produced by increase in the mass flux of the Perseid meteor shower. To estimate the increase in the mass flux ΔF_{imp} we can use a simple formula:

$$\Delta F_{imp} = \frac{M_{ImpProd}}{\tau_{loss}(Na)} \frac{2}{S_{bomb}} \frac{1}{\{Na\}(Y+1)}, \quad (8)$$

where $\tau_{loss}(Na)$ is the lifetime of Na atoms in the exosphere, $S_{bomb}/2$ is the cross-sectional area of the Moon, $\{Na\}$ is the Na mass fraction in the impact-induced hot cloud, Y is the target-toimpactor mass ratio in the cloud. We estimate the lifetime of Na atoms as $1/\tau_{loss}(Na) = 0.9/(2\times\tau_{bal}(Na)) + 0.1/\tau_{ion}(Na)$, where $\tau_{bal}(Na) = 1.3\times10^3$ s is the mean time of ballistic flight

Table 2: Results of spectroscopic search for undetected species in the lunar exosphere on August 12–14, 2009. The values of g-factors are taken from (a): Killen et al. (2009), (b): Sarantos et al. (2012), (c): Sullivan and Hunten (1964), and (d): Flynn and Stern (1996). The dependence of g-factors on radial velocity is considered for Na 5890 and 5896 Å, Ca 4227 Å, Al 3962 Å, Fe 3859 Å, and Ti 3990 Å lines; for other lines g-factors are given at zero Doppler shift. (d) – column densities are calculated for 400 K at the 5 sigma level by Flynn and Stern (1996); the depletion factors are estimated for the case of all mechanisms of delivery of atoms to the exosphere. (e) – column densities obtained by Flynn and Stern (1996) were re-calculated for recently corrected g-values of Si 3906 Å line and Ti 5036 Å line reported by Sarantos et al. (2012), depletion factors are estimated for the case of all mechanisms of delivery of atoms to the exosphere. (f) – Halekas et al. (2013) and (g) – Poppe et al. (2013), depletion factors are estimated for the case of all mechanisms of delivery of atoms to the exosphere. (h) – observations of Cook et al. (2013) at the assumed temperature of 3000 K and [Na]=2.2×10^9 cm^{-2}, depletion factors are estimated for the case of all mechanisms of delivery of atoms to the exosphere. (i) – observations performed on Aug. 12, 23:54 – Aug. 13, 0:24 UT, 2009. Calculations of theoretical brightnesses and depletion factors are performed using the following assumption: $\tau loss(K)=2\times\tau_{bal}(K)$, $\tau_{loss}(K)=2\times\tau_{bal}(K)$, $1/\tau_{loss}(Na)=0.9/(2\times\tau_{bal}(Na))+0.1/\tau_{ion}(Na)$, $1/\tau_{loss}(Li)=0.5/(2\times\tau_{bal}(Na))+0.5/\tau_{ion}(Li)$, for atoms of other elements $\tau_{loss}(X)=\tau_{bal}(X)$ at 3000 K; for all elements $F_{unc}(X) = f_{atom}(X) = 1$. (k) – observations performed on August 13, 2009, 23:22–23:52 UT. Depletion factors are estimated for the case of all mechanisms of delivery of atoms to the exosphere. Calculations of theoretical brightnesses and depletion factors are performed using the same assumptions as for the case (i). (l) – observations performed on Aug. 13, 23:53 – Aug. 14, 0:23 UT, 2009.

Element	λ, Å	g-factor, (photons atom^{-1}s^{-1})	Observed brightness Iobs, (R) (3σ level)		Column density, cm^{-}2			Theoretical brightness I_{theor}, R^h	Depletion factor relative to Na	
			Aug.12, 23: 13–23:43 UT	Aug.13, 23: 22–23:52 UT	This work		N_{zen0}, other works		Our observations	Other data
					$N^i_{zenImp0}$	N^k_{zen0}				
Na	5890	0.59[a]	159	152	4.9×10^8	9.3×10^8	2.2×10^9 [d] 2.3×10^9 [f] 2.2×10^9 [h]	155	1	1
Na	5896	0.34[a]	77	74	4.1×10^8	7.7×10^8	-	90	1	1
K	7699	1.94[b]	-	-	-		1.3×10^9 [d] 4.2×10^9 [f]	30	-	0.06[d] 0.05[f]
Ca	4227	0.59[a]	<13	<10	$<1.1\times10^8$	$<5\times10^7$	$<9.2\times10^7$ [d] $<1.2\times10^9$ [f] $<6.2\times10^8$ [h]	520	>40i >100[k]	>150[d] >10[f] >22[h]
Al	3962	0.035[b]	<13	<9	$<2\times10^9$	$<8.4\times10^8$	$<5.1\times10^9$ [d] $<2\times10^8$ [f] $<10^8$ [g] $<6\times10^7$ [h]	70	>5i >13[k]	>6[d] >150[f] >150[g] >500[h]
Li	6708	16[c]	<30	<24[k]	$<8\times10^6$	$<4.9\times10^6$ [k]	$<1.1\times10^6$ [d]	11	>0.4i >1.6[l]	>20[d]
Fe	3859	0.0041[b]	<15	<15	$<1.9\times10^{10}$	$<1.1\times10^{10}$	$<2.5\times10^{10}$ [d] $<3.8\times10^{10}$ [f] $<1.2\times10^9$ [h]	0.9	>0.06i >0.1[k]	>0.12[d] >0.08[f] >3[h]
Ba	5536	11[d]	<14	<9	$<1.4\times10^7$	$<2.2\times10^6$	$<7.5\times10^6$ [d]	0.6	>0.04i >0.3[k]	>0.25[d]
Ti	3990	0.07[b]	<20	<15	$<1.4\times10^9$	$<6.9\times10^8$	$<4.5\times10^9$ [d,e]	0.5	>0.024i >0.05[k]	>0.02[d,e]
Si	3906	7.9×10^{-5} [b]	<17	<10	$<6.7\times10^{11}$	$<4.2\times10^{11}$	$<3.9\times10^{11}$ [d,e] $<5.8\times10^9$ [f] $<5\times10^7$ [h]	0.25	>0.014i >0.04[k]	>0.12[d,e] >85[f] >1000[h]
Mn	4033	0.0109[b]	<19	<11	$<8.9\times10^9$	$<3.2\times10^9$	$<2.2\times10^9$ [h]	0.04	>0.002i >0.006[k]	>0.02[h]

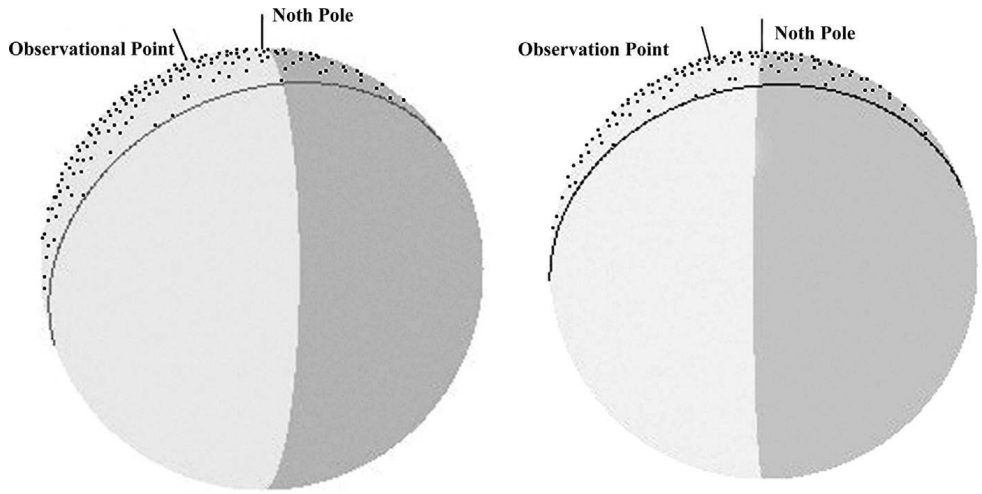

Figure 3: Potential Perseid meteor shower impact region for August 13, 2009, 0 UT (left) and August 14, 2009, 0 UT (right).

of Na atoms at 3100 K, $\tau_{ion}(Na)$ is the Na photoionization lifetime, $6.2{\times}10^4$ s (Huebner et al., 1992), because we assume that impact-produced Na atoms can be seen at observed altitudes just during two ballistic hops (see also Section 4.3 of this paper) while 10% of Na atoms at 3100 K are at escaping orbits and lifetimes of escaping atoms are determined by slow photoionization. According to this estimation, $\tau_{loss}(Na) = 2.88{\times}10^3$ s. The residence time τ_{res} of Na atoms at the surface is equal to 0.7 s at 100 K for adsorption of Na atoms at quartz and rapidly decreases with increasing temperature (Hunten et al., 1988). Since $\tau_{res}(Na) << \tau_{loss}(Na)$, we can neglect the residence time. The north pole of the Moon bombarded by Perseids has a quite low content of Na-rich KREEP basalts and gabbronorites and its average elemental composition corresponds to mixture of ferroan anorthosites and norites with mass ratio of about 1:1 (Berezhnoy et al., 2005). For this reason the elemental composition of the lunar regolith is assumed to be the same as the composition of the mixture of ferroan anorthosites and norites, namely, 0.28 wt% for Na (Lodders and Fegley, 1998). The elemental composition of Perseid meteoroids is assumed to be the same as composition of CI chondrites, namely, 0.5 wt% for Na (Lodders and Fegley, 1998). The target-to-impactor mass ratio Y in the impactinduced hot cloud is assumed to be 50 for the case of 59 km/s impacts of Perseid meteoroids in accordance with Cintala (1992). Thus, the Na mass fraction in the impact-induced hot cloud Na is assumed to be 0.0028. More details about estimation of these values can be found in Berezhnoy and Klumov (2008) and Berezhnoy (2013). Finally, the increase in the mass flux ΔF_{imp} can be estimated with Eq. (8) to be $7.7{\times}10^{-17}$ g cm^{-2} s^{-1} or 27 kg/h. This value corresponds to mass of impacted meteoroids of about 20 kg during the lifetime of Na atoms in the lunar exosphere, about 2900 s.

Because $\tau_{loss}(Na)$ is comparable with duration of performed spectral observations, it is possible to use another model to describe the sharp increase in Na emission, namely, short-time series of impacts at about August 13, 2009, 23:50 min UT.

Assuming a homogeneous distribution of impacts along the section and using Eq. (5), we obtain the same mass impact-produced Na atoms $M_{ImpProd} = 3$ kg, and the impactors can be estimated by a simple formula:

$$M_{Imp} = \frac{M_{ImpProd}}{\{Na\}(Y+1)} \quad (9)$$

Using Eq. (9) we estimate the mass of impactors M_{imp} to be about 20 kg.

Accuracy of our data is not enough to distinguish the model of flux increase and the model of short-time numerous impacts (see Fig. 2). However, the nature of both models is the same, therefore we may consider the estimations of ΔF_{imp} and M_{imp} as two different representation of a single phenomenon of Perseid shower strengthening.

A search for strongest bands of impact-produced diatomic molecules (namely, the 0–0 band of AlO $B^2\Sigma$–$X^2\Sigma$ (4843 Å) and the 0–0 band of MgO $B^1\Sigma^+$–$X^1\Sigma^+$ (4986 Å)) was also performed. Einstein coefficients are equal to $6{\times}10^6$ s^{-1} (Honjou, 2011, 2012) and $2{\times}10^7$ s^{-1} (Daily et al., 2002) for the considered AlO B–X and MgO B–X transitions, respectively. Assuming that the duration of thermal emission is 0.1 s, the electron temperature is 3100 K and that all Al and Mg are present in the form of AlO and MgO molecules, intensities of studied transitions are estimated to be equal to $5{\times}10^{-3}$ and $3{\times}10^{-4}$ R for AlO and MgO, respectively. These values are well below the found upper limits, about 1.2 R for AlO (4843 Å) and 3 R for MgO (4986 Å). Thus, even if these molecules are present in the lunar exosphere, they cannot be detected with this spectroscopic technique.

A search for other emission lines such as Fe (3860 Å), Al (3962 Å), and Ca (4227 Å) in recorded spectra was also performed. Upper limits of the intensitity of expected emission lines are estimated. Fig. 4 shows the "non-detection" of Ca. The same procedure described in Eqs. (1)–(4) is applied for the analysis of emission lines of atoms of other elements. It is assumed that the temperature of atoms of all considered elements is 3100 K. The found upper limits of abundances of atoms of other elements are given in Table 2.

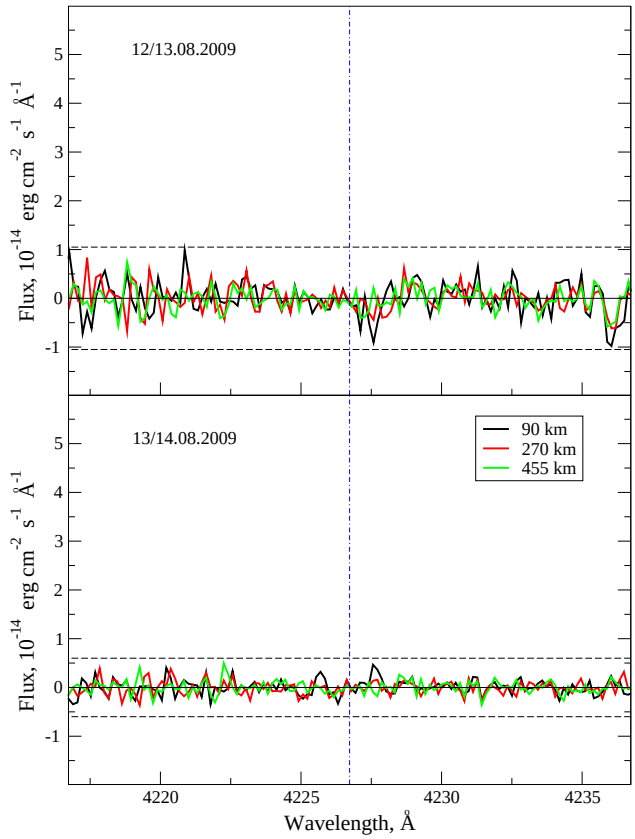

Figure 4: Non-detection of Ca (4227 Å) line in the lunar exosphere.

The theoretical line intensities of atoms of still undetected elements in the lunar exosphere can be also estimated. In accordance with Eq. (2) from (Berezhnoy, 2010), the surface zenith column density $N_{zen0}(X)$ of impact-produced atoms of considered element X can be calculated as

$$N_{zen0}(X) = \frac{F_{ret}\{X\}\tau_{loss}(X)\, f_{atom}(X) F_{unc}(X) F_{imp}(Y+1)}{m(X)} \quad (10)$$

where F_{ret} is the retention factor defined as the mass fraction of the impact-produced cloud captured by the Moon, $\{X\}$ is the mass fraction of element X in the cloud; $\tau_{loss}(X)$ is the lifetime of atoms of X in the exosphere; $F_{unc}(X)$ is the fraction of uncondensed species of element X in the gas phase; F_{imp} is the mass flux of incoming meteoroids in units of g cm^{-2} s^{-1}; and $m(X)$ is the mass of atoms X in grams. The term $f_{atom}(X)$ is the ratio of the abundance of atoms of the element X produced directly during impact and by photolysis to the total abundance of X-containing species in the gas phase of the cloud. In accordance with Berezhnoy (2013), the retention factor F_{ret} is assumed to be 0.6 and the elemental composition of the impact vapor is assumed to be that of mixture of CI chondrite, norite, and ferroan anorthosite with mass ratio equal to 1:25:25. The lifetimes $\tau_{loss}(X)$ of considered atoms in the exosphere were also estimated in accordance with Berezhnoy (2013). Using these assumptions and $F_{unc}(X) = f_{atom}(X) = 1$, theoretical brightnesses of atomic lines of different elements for the case of the Perseid mass flux of 27 kg/h are estimated and summarized in Table 2.

4. Discussion

4.1. Other sources of Na atoms in the exosphere

Intensities of solar wind and solar X-rays on August 12/13 and 13/14, 2009 are comparable (Solar monitor, 2009; OMNI, 2009). Table 3 lists the solar radio flux at 10.7 cm and the solar wind density and velocity at the time of observations. The last two data are related to ion sputtering and high values would indicate high rates; F10.7 index, instead, is a proxy for the solar UV activity, hence also of the photon stimulated desorption efficiency. All these values are clearly in the usual ranges. For example, the five minute average values of the solar wind density during both nights are roughly constant within 20% and always below 4 cm^{-3}. High-speed streams or highly compressed regions (such as coronal mass ejections or co-rotating interaction regions) were not observed at 1 AU, and the space weather was rather calm during those days (ACE-SWEPAM, 2009). Meanwhile, we cannot exclude possible influence of some factors in the solar wind on the discussed phenomenon, which should be investigated in the future. Changing illumination conditions leads to a higher rate of photon-simulated desorption of line-of-sight Na atoms from the surface to the lunar exosphere on August 12/13 as compared to August 13/14, 2009. However, illumination conditions are changed too slowly to explain sudden changes of Na column density during several hours.

Let us assume that activity of the Perseid shower on the Moon was the same as that on Earth at the same time; in fact, 59 km/s Perseid meteoroids cross the distance between Earth and the Moon in about 100 min and the Moon was near the last quarter. Maxima of the Perseid meteor shower on Earth occurred on August 12, 2009 at 8 and 18 UT and August 13, 2009, 6 UT. According to IMO (2009), the activity of Perseid 2009 meteor shower on Earth in units of zenithal hourly rate (the number of meteors a single observer would see in one hour under a clear, dark sky if the radiant of the shower were at the zenith) was equal to 65 and 25 on August 12, 23 UT – August 13, 1 UT and August 13, 23 UT – August 14, 2009, 1 UT, respectively. Thus, we expect a related enrichment of the content of impact-produced Na atoms in the lunar exosphere on August 12/13, 2009. Moreover, at the time of performed observations only the intensity of micrometeorite bombardment changes significantly, while other sources of the Na lunar exosphere (ion sputtering and photon-induced desorption) remain almost constant.

4.2. Accuracy of estimation of mass of impacted Perseid meteoroids

Let us estimate the accuracy of our estimation of total mass of impacting meteoroids. Taking into consideration uncertanties of the estimation of the temperature of Na atoms, the accuracy of the Na column density is estimated to be about 50meteoroids could occur at Na-rich regions. In fact the Na content in the lunar rocks is variable, from 0.27 wt% in ferroan anorthosites and 0.3 wt% in norites to 0.7 wt% in gabbronorites

and KREEPbasalts (Lodders and Fegley, 1998). Deposits of Na in the atomic form are located at the poles of the Moon. About 1.5 kg of Na atoms were released to the impact-produced plume above the south pole of the Moon after the LCROSS impact in the crater Cabeus (Killen et al., 2010). Assuming mass of the plume of about 3000 kg (Colaprete et al., 2010), this amount corresponds to about 0.05 wt% of Na content at the south pole of the Moon. As a volatile element, Na is enriched in the impact-produced cloud as compared to that in the lunar regolith (Gerasimov et al., 1998; Yu and Hewins, 1998). Both factors may lead to overestimation of mass of impacted Perseid meteoroids. Additional significant uncertainty may appear due to poor accuracy of estimations of duration of Perseid meteoroid peak activity, lifetime of Na atoms in the lunar exosphere, the target-to-impactor mass ratio in the impactproduced cloud, and the k_{geom} value. In summary, total mass of impacted Perseid meteoroids during the lifetime of Na atoms in the lunar exosphere, about 2900 s, is estimated with an accuracy of about a factor of three, to the range between 7 and 70 kg. Let us note that according to estimates of the Perseid mass flux on the Earth (Hughes and McBride, 1989), the total mass flux of Perseid meteoroids colliding with the Moon is about 1 kg/h; this value is significantly lower than our estimate.

4.3. Single big impact or numerous small impacts?

To analyze the spectral observations a model of numerous impacts of small meteoroids (see Eq. (7)) was used. Another possibility is to model the unique impact of a big meteoroid. The probability of impact of a 300 kg (80 cm in diameter) sporadic meteoroid (for this case Y= 3, see Eq. (10)) required to explain the changes of properties of Na atmosphere of the Moon can be estimated as the ratio between the duration of our observations and the frequency of required collisions. Frequency of collision of a required 80 cm sporadic meteoroid is about one event per week on Earth (Brown et al., 2002); the probability of such impact during our observations on August 12/13, 2009 is estimated as low as $5{\times}10^{-4}$ h^{-1}. Based on recent observations of impact events, this value is estimated as high as $5{\times}10^{-3}$ h^{-1} (Ortiz et al., 2006; Brown et al., 2013; Madiedo et al., 2014). However, even higher collision rate of sporadic meteoroids cannot explain observed significant quick changes of the Na surface zenith column density. Presence of massive bodies in meteor streams is characterized by the mass distribution index *s*. Namely, if the *s* value is less than 2, the majority of mass is concentrated in several big bodies. In the opposite case, it is concentrated in small numerious meteoroids. Hypothesis of the single impact of a big meteoroid is in agreement with average mass distribution index of 1.45 found through radar observations of the Perseid showers of 1980–1983, 1985, 1986, 1989, 1991–1993, 1995, 1996, 2000 (Pecinová and Pecina, 2007). Other radar observations give slighly higher *s* value equal to 1.61 (Šimek, 1987). Estimations of the spatial number density of Perseid meteoroids with diameters of 0.03 mm (Brown and Rendtel, 1996), 1 cm (Beech and Illingworth, 2001), and 3 m (Smirnov and Barabanov, 1997) and results of Beech et al. (2004) agree with the Perseid meteor shower mass distribution index of about 1.6–1.8. Based on Fig. 2 of Beech et al. (2004) at the assumed $s = 1.7$, the frequency of collisions of 30 cm Perseid meteoroids with the Moon is estimated as several impacts per hour during maximum of the Perseid meteor shower.

However, Apollo seismograms in 1975 detected an impact rate of small (about 0.1–1 kg) Perseid meteoroids of about 5 events per day, while large meteoroids (41 kg) were not detected in 1972– 1976 and only the upper limit of the impact rate of such meteoroids is estimated as about 0.5 events per day (Oberst and Nakamura, 1991). Only a unique optical flash at the surface of the Moon caused by Perseid meteoroid is detected (Yanagisawa et al., 2006). Mass of the impacted meteoroid, about 12 g, and duration of performed observations agree with low frequency of impacts of large Perseid meteoroids (41 kg) estimated by Oberst and Nakamura (1991). The works of Oberst and Nakamura (1991) and Yanagisawa et al. (2006) can be explained if the *s* value is about 2.0 or higher. In this case the frequency of 30 cm Perseid meteoroid impacts can be estimated as low as $3{\times}10^{-3}$ h^{-1}.

One of the possible reasons of significant uncertainty of the impact rate of big Perseid meteoroids is that the *s* value depends on time. For example, radar observations give the *s* value range between 1.3 and 1.6 during different years Pecinová and Pecina (2007). These changes may be also responsible for variable impact rates of massive Perseid meteoroids reported by Oberst and Nakamura (1991).

Based on our observations, it is possible to try to distinguish scenarios of the unique impact of big meteoroids, short-time series of small impacts, and increases in the Perseid mass flux (see Fig. 2). Namely, after the big unique impact and short-time series of small impacts, the temperature of impact-produced Na atoms will decrease quickly while for the case of an increase in the mass flux it remains constant. Assuming the energy accommodation coefficient $\chi = 0.62$ for sodium (Hunten et al., 1988), the surface temperature of 350 K, and the initial temperature of Na atoms of 3000 K, the effective temperature will be equal to 1350, 730, and 500 K after a first, second, and third collision of Na atoms with the surface, respectively, occurring about 21, 35, and 45 min after the impact, respectively. These temperatures correspond to scale heights equal to 670, 300, 160, and 110 km, respectively. It may lead to the significant decrease of the amount of detected Na atoms at 455 km altitude during recording of the third spectrum if single impact or short-time bombardment by small meteoroids occurred between August 12, 23:40 UT and August 13, 0:15 UT. Thus, almost equal column densities of Na atoms estimated from second and third spectra can be better explained by increase in the mass flux of small meteoroids. However, if the value is significantly lower than 0.6 as discussed by Smyth and Marconi (1995), then hypotheses of unique impact or short-time bombardment by small meteoroids are still valid if it occurred exactly at the middle of the second spectrum of August 12/13, 2009 which seems to be unlikely as discussed above.

4.4. The presence of atoms of refractory elements in the lunar exosphere

In our observations the depletion factor I_{theor}/I_{obs} is defined as the ratio of predicted theoretical intensity I_{theor} to the ob-

served upper limits I_{obs} of the emission intensity of the atoms in study at a given altitude at the 3 sigma level. The estimated lower limits of depletion factors of refractory elements depends on altitude and time of performed observations. Namely, for all mechanisms of delivery of the atoms in study to the lunar exosphere lower limits of depletion factors were maximal for the first spectrum recorded on August 13/14, 2009. For the impact delivery, the lower limits of depletion factors were maximal for the second spectrum recorded on August 12/13, 2009, because at this period of time the Perseid meteoroid mass flux was maximal. The upper limits of Ca and Al column densities are significantly lower than those estimated using Eq. (10) in assumption that $F_{unc}(X) = f_{atom}(X) = 1$ (see Table 2, observed vs theoretical brightness). This result can be explained if $F_{unc}(X) f_{atom}(X) << 1$ for Al and Ca. Depletion of abundances of impact-produced atoms of refractory elements such as Ca and Al in the lunar exosphere occurs due to formation of slowly photolyzed molecules and condensation of dust particles in the cooling impact-produced cloud (Berezhnoy, 2013). Several other authors also estimated upper limits of refractory elements in the lunar exosphere (see Table 2). However, these observations were performed in the absence of major meteor showers and include information about different sources of atoms of refractory elements in the lunar exosphere including sporadic meteoroids and solar photons. Using Eqs. (1) and (4) from (Berezhnoy, 2013), for the case of all mechanisms of atom delivery in the lunar exosphere and assuming [Na]=2.2×10^9 cm^{-2}, lower limits of depletion factors regarding Na for observations of Flynn and Stern (1996), Halekas et al. (2013), Cook et al. (2013) are also estimated (see Table 2). As compared to these results, our observations give stringent upper limits of the column density for Ca, Ba, and Ti atoms (see Table 2). Our observations also give a comparable limit of depletion factors for Ca atoms as compared to the previous best estimate of Flynn and Stern (1996) while Cook et al. (2013) gave stronger constraints on behavior of Al, Si and Fe atoms in the lunar exosphere. As for Li and Ba, our obtained upper limits of the column densities are comparable with estimated theoretical values while the theoretical upper limits of the column densities of Fe, Ti, and Mn atoms are significantly lower than the obtained upper limits even at the most favorite case of $F_{unc}(X) f_{atom}(X) = 1$.

5. Conclusions

Increase in the zenith surface column density of Na atoms in the lunar exosphere on August 13, 2009 at 0–1 UT of about 40detected while observations of August 13/14, 2009 show the almost constant surface column density of Na atoms estimated from all three recorded spectra. Our observations can be better explained by numerous collisions of small Perseid meteoroids (< 1 kg) with the Moon (the mass flux is about 27 kg/h) with respect of single impact hypothesis (mass of unique meteoroid of about 20 kg). New stringent upper limits of Ca, Ba, and Ti column densities in the lunar exosphere are obtained. Lower limits of depletion factors of Ca and Al atoms in the lunar exosphere during maximum of the Perseid meteor shower are estimated for the first time and explained by formation of silicate dust particles during cooling of an expanded impact-produced cloud. Our observations confirm influence of the meteoroid bombardment on the properties of the lunar exosphere. More observations of the lunar exosphere during activity of meteor showers are required for deeper understanding of these phenomena.

Acknowledgments

Authors thank S.F. Velichko (Terskol Observatory) for performing the observations and T.K. Churyumova, A.Ya. Freidzon, O.V. Khabarova, A.M. Mozgova, P. Pecina, and anonymous referee for helpful suggestions.

References

ACE-SWEPAM, 2009, (http://www.srl.caltech.edu/ACE/ASC/level2/index.html) Barbieri, C., Benn, C.R., Cremonese, G., Verani, S., Zin, A., 2001. Meteor showers on the lunar atmosphere. Earth Moon Planets 85–86, 479–486.

Beech, M., Illingworth, A., 2001. 2001 Perseid fireball observations. WGN, J. Int. Meteor Org. 29, 181–184.

Beech, M., Illingworth, A., Brown, P., 2004. A telescopic search for large Perseid meteoroids. Mon. Not. R. Astron. Soc. 348, 1395–1400.

Berezhnoy, A.A., Hasebe, N., Kobayashi, M., Michael, G.G., Okudaira, O., Yamashita, N., 2005. A three end-member model for petrologic analysis of lunar prospector gamma-ray spectrometer data. Planet. Space Sci. 53, 1097–1108.

Berezhnoy, A.A., Klumov, B.A., 2008. Impacts as a source of the atmosphere on Mercury. Icarus 195, 511–522.

Berezhnoy, A.A., 2010. Meteoroid bombardment as a source of the lunar exosphere. Adv. Space Res. 45, 70–76.

Berezhnoy, A.A., 2013. Chemistry of impact events on the Moon. Icarus 226, 205–211.

Brown, P., Rendtel, J., 1996. The Perseid meteoroid stream: characterization of recent activity from visual observations. Icarus 124, 414–428.

Brown, P., Spalding, R.E., ReVelle, D.O., Tagliaferri, E., Worden, S.P., 2002. The flux of small near-Earth objects colliding with the Earth. Nature 420, 294–296.

Brown, P.G., Assink, J.D., Astiz, L., Blaauw, R., Boslough, M.B., Borovička, J., Brachet, N., Brown, D., Campbell-Brown, M., Ceranna, L., Cooke, W., de Groot-Hedlin, C., Drob, D.P., Edwards, W., Evers, L.G., Garces, M., Gill, J., Hedlin, M., Kingery, A., Laske, G., Le Pichon, A., Mialle, P., Moser, D.E., Saffer, A., Silber, E., Smets, P., Spalding, R.E., Spurn, P., Tagliaferri, E., Uren, D., Weryk, R.J., Whitaker, R., Krzeminski, Z, 2013. A 500-kiloton airburst over Chelyabinsk and an enhanced hazard from small impactors. Nature 503, 238–241.

Burger, M.H., Killen, R.M., McClintock, W.E., Vervack Jr., R.J., Merkel, A.W., Sprague, A.L., Sarantos, M., 2012. Modeling MESSENGER observations of calcium in Mercury's exosphere. J. Geophys. Res. 117 (CiteID E00L11) (15 pp.), http://dx.doi.org/10.1029/2012JE004158

Chamberlain, J.W., 1963. Planetary coronae and atmospheric evaporation. Planet Space Sci. 11, 901–960.

Chamberlain, J.W., Hunten, D.M., 1987. Theory of Planetary Atmospheres. Academic Press, Orlando p. 481

Churyumov, K.I., Berezhny, O.O., Ponomarenko, V.O., Baransky, O.R., Churyumova, T.K., Kleshchenok, V.V., Mozgova, A.M., Kovalenko, N.S., Shevchenko, V.V., Kozlova, E.A., Pakhomov, Yu.V., Velikodsky, Yu.I., 2012. Observations of the non-stationary atmosphere of the Moon and some its parameters. Astron. School's Rep. 8, 175–181 (in Ukrainian).

Cintala, M., 1992. Impact-induced thermal effects in the lunar and Mercurian regoliths. JGR 97, 947–973.

Colaprete, A., Schultz, P., Heldmann, J., Wooden, D., Shirley, M., Ennico, K., Hermalyn, B., Marshall, W., Ricco, A., Elphic, R.C., Goldstein, D., Summy, D.,

Bart, G.D., Asphaug, E., Korycansky, D., Landis, D., Sollitt, L., 2010. Detection of water in the LCROSS ejecta plume. Science 330, 463–468. Cook, J.C., Stern, S.A., Feldman, P.D., Gladstone, G.R., Retherford, K., Tsang, C.C.C., 2013. New upper limits on numerous atmospheric species in the native lunar atmosphere. Icarus 225, 681–687.

Daily, J.W., Dreyer, C., Abbud-Madrid, A., Branch, M.C., 2002. Transition probabilities in the $B^1\Sigma^+$–$X^1\Sigma^+$ and the $B^1\Sigma^+$–$A^1\Pi$ electronic systems of MgO. J. Mol. Spectrosc. 214, 111–116.

Flynn, B., Mendillo, M., 1993. A picture of the moon's atmosphere. Science 261, 184–186.

Flynn, B.C., Stern, S.A., 1996. A spectroscopic survey of metallic species abundances in the lunar atmosphere. Icarus 124, 530–536.

Gerasimov, M.V., Ivanov, B.A., Yakovlev, O.I., Dikov, Yu.P., 1998. Physics and chemistry of impacts. Earth Moon Planets 80, 209–259.

Goldstein, D.B., Austin, J.V., Barker, E.S., Nerem, R.S., 2001. Short-time exosphere evolution following an impulsive vapor release on the Moon. J. Geophys. Res. 106 (E12), 32841–32845.

Halekas, J.S., Poppe, A.R., Delory, G.T., Sarantos, M., McFadden, J.P., 2013. Utilizing ARTEMIS pickup ion observations to place constraints on the lunar atmosphere. J. Geophys. Res. 118, 81–88.

Honjou, N., 2011. Ab initio study of band strengths for the $F^2\Sigma^+$–$A^2\Pi$ electronic transition of AlO. Comput. Theoret. Chem. 978, 138–142.

Honjou, N., 2012. (private communication).

Huebner, W.F., Keady, J.J., Lyon, S.P., 1992. Solar photo rates for planetary atmospheres and atmospheric pollutants. Astrophys. Space Sci. 195 (1–289), 291–294.

Hughes, D., McBride, N., 1989. The mass of meteoroid streams. Mon. Not. R. Astron. Soc. 240, 73–79.

Hunten, D.M., Shemansky, D.E., Morgan, T.M., 1988. The Mercury atmosphere. In: Vilas, F., Chapman, C., Matthews, M. (Eds.), Mercury. University of Arizona Press, Tucson, AZ, pp. 562–612

Hunten, D.M., Cremonese, G., Sprague, A.L., Hill, R.E., Verani, S., Kozlowski, R.W.H., 1998. The Leonid meteor shower and the lunar sodium atmosphere. Icarus 136, 298–303.

Hunten, D.M., Kozlowski, R.W.H., Sprague, A.L, 1991. A possible meteor shower on the Moon. Geophys. Res. Lett. 18, 2101–2104.

IMO, 2009. Perseids 2009: Visual Data Quicklook. (http://www.imo.net/live/perseids2009)

Killen, R.M., Shemansky, D., Mouawad, N., 2009. Expected emission from Mercury's exospheric species, and their ultraviolet–visible signatures. Astrophys. J. Suppl.Ser. 181, 351–359.

Killen, R.M., Potter, A.E., Hurley, D.M., Plymate, C., Naidu, S., 2010. Observations of the lunar impact plume from the LCROSS event. Geophys. Res. Lett. 37 (CiteID L23201).

Lodders, K., Fegley, B., 1998. The Planetary Scientist Companion. Oxford University Press, New York, p. 371

Madiedo, J.M., Ortiz, J.L., Morales, N., Cabrera-Cao, J., 2014. A large lunar impact blast on 2013 September 11. Mon. Not. R. Astron. Soc. 439, 2364–2369.

Mendillo, M., Baumgardner, J., Flynn, B., 1991. Imaging observations of the extended sodium atmosphere of the Moon. Geophys. Res. Lett. 18, 2097–2100.

Mendillo, M., Flynn, B., Baumgardner, J., 1993. Imaging experiments to detect an extended sodium atmosphere on the Moon. Adv. Space Res. 13, 313–319.

Mendillo, M., Baumgardner, J., Wilson, J., 1999. Observational test for the solar wind sputtering origin of the Moon's extended sodium atmosphere. Icarus 137, 13–23.

Oberst, J., Nakamura, Y., 1991. A search for clustering among the meteoroid impacts detected by the Apollo lunar seismic network. Icarus 91, 315–325.

OMNI, 2009. (http://omniweb.gsfc.nasa.gov) Ortiz, J.L., Aceituno, F.J., Quesada, J.A., Aceituno, J., Fernández, M., Santos-Sanz, P., Trigo-Rodríguez, J.M., Llorca, J., Martín-Torres, F.J., Montañés-Rodríguez, P., Pallé, E., 2006. Detection of sporadic impact flashes on the Moon: implications for the luminous efficiency of hypervelocity impacts and derived terrestrial impact rates. Icarus 184, 319–326.

Pecinová, D., Pecina, P., 2007. Radar meteors range distribution model. II. Shower flux density and mass distribution index. Contrib. Astron. Obs. Skaln. Pleso 37, 107–124.

Poppe, A.R., Halekas, J.S., Samad, R., Sarantos, M., Delory, G.T., 2013. Model-based constraints on the lunar exosphere derived from ARTEMIS pickup ion observations in the terrestrial magnetotail. J. Geophys. Res. 118, 1135–1147.

Potter, A.E., Morgan, T.H., 1988. Discovery of sodium and potassium vapor in the atmosphere of the Moon. Science 241, 675–680.

Sarantos, M., Killen, R.M., Sharma, A.S., Slavin, J.A., 2008. Influence of plasma ions on source rates for the lunar exosphere during passage through the Earth's magnetosphere. Geophys. Res. Lett. 35 (CiteID L04105).

Sarantos, M., Killen, R.M., Sharma, A.S., Slavin, J.A., 2010. Sources of sodium in the lunar exosphere: modeling using ground-based observations of sodium emission and spacecraft data of the plasma. Icarus 205, 364–374.

Sarantos, M., Killen, R.M., McClintock, W.E., Bradley, E.T., Vervack, R.J., Benna, M., Slavin, J.A., 2011. Limits to Mer-

cury's magnesium exosphere from MESSENGER second flyby observations. Planet. Space Sci. 59, 1992–2003.

Sarantos, M., Killen, R.M., Glenar, D.A., Benna, M., Stubbs, T.J., 2012. Metallic species, oxygen and silicon in the lunar exosphere: upper limits and prospects for LADEE measurements. J. Geophys. Res. 117 (CiteID A03103).

Šimek, M., 1987. Dynamics and evolution of the structure of five meteor streams. Bull. Astron. Inst. Czech. 38, 80–91.

Smirnov, M.A., Barabanov, S.I., 1997. The optical observations of meteoroids in nearEarth space. In: Proceedings of 2nd European Conference on Space Debris. ESA SP-393, ESOC, Darmstadt, Germany. pp. 155–157.

Smith, S.M., Wilson, J.K., Baumgardner, J., Mendillo, M., 1999. Discovery of the distant lunar sodium tail and its enhancement following the Leonid meteor shower of 1998. Geophys. Res. Lett. 26, 1649–1652.

Smyth, W.H., Marconi, M.L., 1995. Theoretical overview and modeling of the sodium and potassium atmospheres of the Moon. Astrophys. J. 443, 371–392.

Solar Monitor, 2009. (http://www.solarmonitor.org)

Space Weather, 2009. (http://www.spaceweather.ca/data-donnee/sol_flux/sx-5eng.php)

Sprague, A.L., Hunten, D.M., Kozlowski, R.W.H., Grosse, F.A., Hill, R.E., Morris, R.L., 1998. Observations of sodium in the lunar atmosphere during International Lunar Atmosphere Week, 1995. Icarus 131, 372–381.

Sprague, A.L., Sarantos, M., Hunten, D.M., Hill, R.E., Kozlowski, R.W.H., 2012. The lunar sodium atmosphere: April–May 1998. Can. J. Phys. 90, 725–732.

Stern, S.A., Parker, J.W., Morgan, Th.H., Flynn, B.C., Hunten, D.M., Sprague, A., Mendillo, M., Festou, M.C., 1997. NOTE: an HST search for magnesium in the lunar atmosphere. Icarus 127, 523–526.

Sullivan, H.M., Hunten, D.M., 1964. Lithium, sodium and potassium in the twilight airglow. Canadian Journal of Physics 42, 937–956.

Tug, H., 1977. Vertical extinction on La Silla. ESO Messenger 11, 7–8. Verani, S., Barbieri, C., Benn, C., Cremonese, G., 1998. Possible detection of meteor stream effects on the lunar sodium atmosphere. Planet. Space Sci. 46, 1003–1006.

Verani, S., Barbieri, C., Benn, C.R., Cremonese, G., Mendillo, M., 2001. The 1999 Quadrantids and the lunar Na atmosphere. Mon. Not. R. Astron. Soc. 327, 244–248.

Yanagisawa, M., Ohnishi, K., Takamura, Y., Masuda, H., Sakai, Y., Ida, M., Adachi, M., Ishida, M., 2006. The first confirmed Perseid lunar impact flash. Icarus 182, 489–495.

Yu, Y., Hewins, R.H., 1998. Transient heating and chondrule formation: evidence from sodium loss in flash heating simulation experiments. Geochim. Cosmochim. Acta 62, 159–172.